JASS Journal of Astronomy and Space Sciences

The First Comprehensive Photometric Study of the Neglected Binary System V345 Cassiopeiae

Min-Ji Jeong, Chun-Hwey Kim[†]

Department of Astronomy & Space Science, Chungbuk National University, Cheongju 361-763, Korea

We present the first *BVRI* CCD photometric observations of V345 Cas made on 22 nights during the observing seasons in 2007-2008. Our light curves, resembling those of EB-type binary stars, are analyzed with the 2003 version of the Wilson-Devinney binary code. The photometric study shows that V345 Cas is a typical semi-detached binary system with the primary star being about ΔT = 2400 K hotter, two times more massive, but only 17% larger than the secondary star being filled with it's Roche-lobe. The orbit has a relatively large inclination of about 88°. A cool spot on the secondary component is modeled to explain a small light curve asymmetry. Absolute dimensions and related radiometric parameters of the eclipsing pair are calculated and their evolutionary states are discussed with the HR diagrams of mass-radius and temperature-luminosity. A period analysis of all available times of minima, including our measurements, indicates that the orbital period may vary in a cyclical way, unfortunately the secondary period for the variation can not be uniquely determined because of lack of present timing data.

Keywords: eclipsing binary star, V345 Cassiopeiae, photometric solution, cool spot, fundamental parameters, evolutionary status

1. INTRODUCTION

The light variability of V345 Cas (AN 190.1943, 2MASS J23083986+5406545, USNO B1.0 1441-0442463) was discovered by Hoffmeister (1943). Huth (1956) classified the system as a β Lyr-type eclipsing binary showing the light-variation of 13.^{m}1 to 14.^{m}2. He also determined the first light elements as *Min I* = HJD 2428835.307 + 0.^{d} 6887589*E*. Since his study numerous times of minimum light were published by many investigators (see Table 3 for the references). By using all the times of minimum light available to them, Kreiner et al. (2001) gave an ephemeris (*Min I* = HJD 2428835.3107 + 0.^{d}68875832*E*). Neither any light curves nor radial velocity curves have been published so far.

As reviewed above, V345 Cas is a neglected binary system whose photometric properties were less known. Thus we have included V345 Cas in our target stars to study photometric properties of close binary stars. In this paper we present, for the first time, two sets of *BVRI* light curves

of V345 Cas secured in 2007-2008, and analyze them to obtain the global photometric properties as well as the dynamical behavior of the orbital period. Also we estimate the absolute dimensions of V345 Cas, and finally we discuss the evolutionary status of two components in the system.

2. OBSERVATIONS AND LIGHT CURVES

2.1 Observations

Our photometric observations were made on 22 nights in the 2007-2008 observing seasons with a FLI 2K CCD camera and a Johnson's standard *BVRI* filter set attached to a 1-m reflecting telescope at Mt. Lemon Astronomical Observatory (LOAO) in Arizona, USA. The telescope was controlled remotely at the Korea Astronomy and Space Science Institute (KASI). The CCD camera, which is thermo-electrically cooled during the observations, has the field

Table 1. The coordinates and magnitudes of variable, comparison and check stars.[†]

Star	Catalogue (USNO-B1.0)	α (J2000)	δ (J2000)	B (mag)	R (mag)
Variable	1441-0442463	$23^h08^m39.^s863$	$+54°06'54''.57$	13.88	13.24
Comparison	1440-0439477	$23^h08^m24.^s696$	$+54°05'04''.91$	15.03	14.03
Check	1440-0439661	$23^h08^m41.^s504$	$+54°03'46''.22$	14.92	14.01

[†]All data were extracted from the USNO-B catalog (see Monet et al. 2003)

of view of about 20.'5 × 20.'5 at the f/7.5 Cassegrain focus of the telescope. Each of the frames was 2 × 2 binned and differently exposed from 30 s to 140 s according to the filters used and weather conditions of each nights. All measured frames were corrected with bias, dark, and flat-field images and preprocessed in the IRAF/DIPHO S/W package. The IRAF Apphot was used to determine instrumental magnitudes. The USNO B1.0 1440-0439477 and USNO B1.0 1440-0439661 near V345 Cas were chosen as a comparison and check stars, respectively. Table 1 lists the coordinates and photometric characteristics of V345 Cas, comparison and check stars and Fig. 1 shows one of the observed CCD frames where the program stars are indicated. Differential magnitudes of the check star relative to the comparison star show that our mean photometric accuracy during the observations is about 0.01 mag in all *BVRI* bandpasses. A total of 862 measurements (*B*: 230, *V*: 230, *R*: 200, and *I*: 202) in 2007 and 1020 (*B*: 253, *V*: 255, *R*: 261, and *I*: 251) in 2008 were secured. All individual observations are available on request from the second author. Two sets of complete *BVRI*
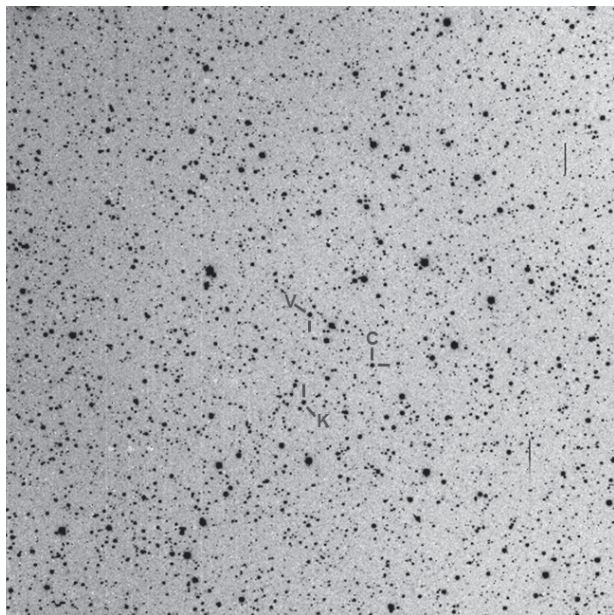

Fig. 1. The finding chart of V345 Cas. The field of view is about 22.5' × 22.5'. 'V', 'C' and 'K' denote V345 Cas, the comparison (USNO B1.0 1440-0439477) and check (USNO B1.0 1440-0439661) stars, respectively. East is left and north is up.

light and color curves were shown in Fig. 2 where the phase was calculated with a new light elements as follows;

$$Min.\ I = HJD\ 2451166.2152\ (\pm0.0021) + 0.^d68876134\ (\pm0.00000037)E. \qquad (1)$$

Eq. (1) was determined with a least-squares method by using recent 21 times of minima of which the (O-C) residuals show a linear pattern to fit well to our observations.

2.2 Light curves

As shown in Fig. 2, two sets of *BVRI* light curves of V345 Cas are consistent each other and have deep eclipses in the primary minimum and shallow in the secondary, similar to other short-period Algol-type eclipsing binaries (e.g., CL Aur (Lee et al. 2010), SW Lyn (Kim et al. 2010) and RU UMi (Lee et al. 2008)). The depth of the primary eclipse decreases with wavelength, being equal to about $1.^m42$, $1.^m30$, $1.^m23$ and $1.^m11$ for *B*, *V*, *R*, and *I*, respectively. However, the depth of the secondary eclipse increases with wavelength, being equal to about $0.^m23$, $0.^m25$, $0.^m30$ and $0.^m33$ for *B*, *V*, *R* and *I*, respectively. Another interesting feature is that all color curves of *B-V*, *V-R* and *R-I* show redder during the primary eclipse and bluer during the secondary eclipse. These two phenomena (wavelength-dependence of eclipse depth and opposite color variations at the primary and secondary eclipses) would be strong indications that 1) primary eclipse is an occultation (Sipahi 2005) and 2) temperature difference between two components is relatively large. In addition it is seen that there is a small asymmetry between the descending and the ascending branches during secondary eclipse. The descending branch is more sharp than the ascending one and the asymmetry is more pronounced as the wavelength is shorter. Furthermore the ascending branches in the 2007 light curves are lower than those in the 2008 light curves, indicating that the asymmetry is time-variable.

3. LIGHT CURVE SYNTHESIS

As explained in the previous section, there is a small difference due to light curve asymmetry and its variation between the 2007 and 2008 light curves. Therefore we solved two sets of filtered light curves separately with the 2003 version of the Wilson-Devinney binary code (hereafter WD, Wilson & Devinney 1971, van Hamme & Wilson 2003). Unfortunately, we have no information on the temperature of the primary star (T_1) as well as the mass ratio ($q = M_2/M_1$),
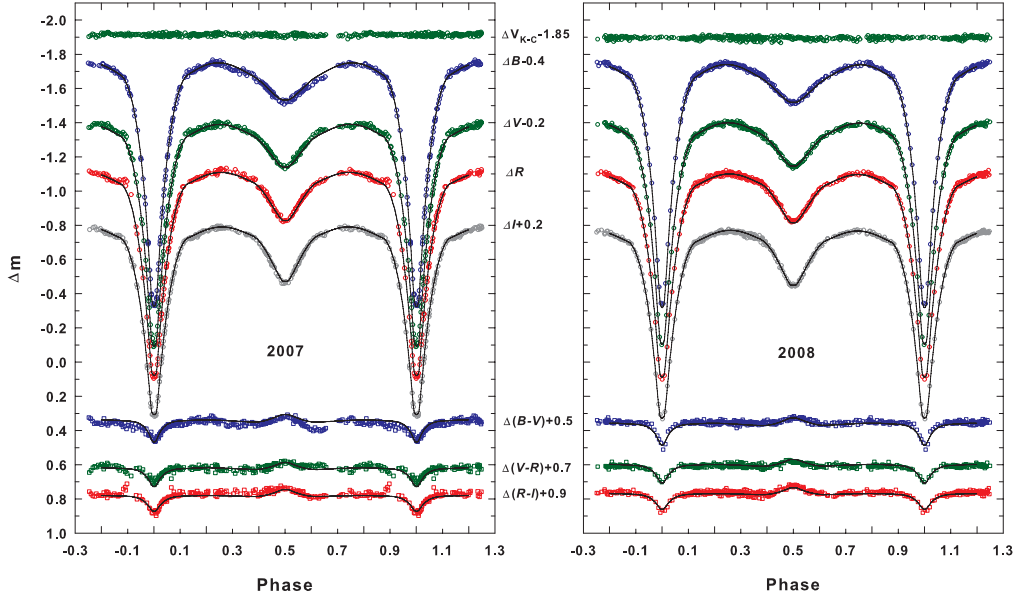
Fig. 2. The observed two sets of *BVRI* light and color curves of V345 Cas. Left: the 2007 light curves, right: the 2008 ones. The light curves of comparison minus check stars are plotted in the top of both panels. The solid curves denote the theoretical model light and color curves.

although these parameters are very essential to any light curve synthesis based on a Roche geometry (such as the WD code) which is sensitive to them. In order to estimate the temperature of the primary star which is eclipsed at primary eclipse, we collected information on magnitudes measured at various bandpasses from some catalogues. From the magnitude data we calculated color indices and estimated temperatures corresponding to each of the color indices by using the Allen's tables (Cox 2000). These are listed in Table 2. The resultant temperatures of the V345 Cas system are distributed in the wide range from 6548 K to 17273 K. So the temperatures were averaged to be 7366 K when the unreasonably large temperatures of 11042 K from GSC2.3 catalog and 17273 K from NOMAD-1 were excluded. It may be hasty to use the averaged temperature of 7366 K as the temperature of the primary star because it was obtained from too much widely distributed temperatures. Thus, by using our 2008 light curves, a temperature-searching (hereafter *T*-search) of the primary star with the WD code was intensively made for both of cases that the primary star

has a radiative envelope or a convective envelope, because the averaged temperature is near the boundary of the two cases. The result of our *T*-search for a series of models with varying temperature was shown in the upper panel of Fig. 3 where open squares with lines represent the case with a radiative envelope and open circles a convective envelope. For the radiative models the weighted sum of the squared residuals, $\Sigma W (O\text{-}C)^2$ (hereafter Σ) has a global minimum at T_1 = 7400 K while no convergence of the Σ was achieved for the convective cases, indicating that the primary star has a radiative envelope. It is very impressive to note that the temperature obtained with the *T*-search is practically the same as that averaged from the catalogues. As a next step, after fixing the temperature of the primary star as T_1 = 7400 K, we made an intensive *q*-search which shows to have a global convergence at *q* = 0.5, as shown in the lower panel of Fig. 3. In these procedures, the differential correction (DC) program of the WD code started from mode 2 (detached system) but always converged to mode 5 (semi-detached system with the secondary component being filled with it's inner Roche lobe) during the computation. Therefore subsequent light curve syntheses were made with mode 5, employing the method of multiple subsets (Wilson & Biermann 1976) to ensure the stability of our solutions. Gravity darkening and albedo coefficients were adopted as g_1 = 1.00 and g_2 = 0.32 (Lucy 1967) and A_1 = 1.0 and A_2 = 0.5 (Rucinski 1969), respectively. Here, the subscript "1" denotes the hotter and massive primary star. The limb-darkening (LD) coefficients from the logarithmic law were

Table 2. Color indices and temperatures of V345 Cas extracted from various catalogs.

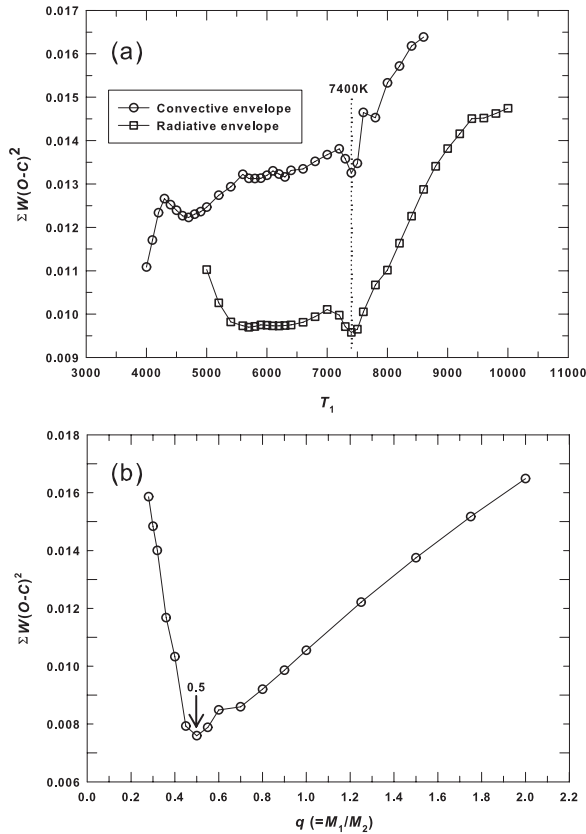| Catalogue[†]	*B-V*	*B-R*	*J-H*	Temperature
USNO-B1.0	-	0.64	-	7180
USNO-B1.0	-	0.84	-	6650
GSC2.3	-0.09	-	-	11042
USNO-A2.0	-	0.2	-	8681
2MASS	-	-	0.225	6548
NOMAD-1	0.22	-0.27	-	7769, 17273

[†]http://vizier.u-strasbg.fr/

Fig. 3. (a) The *T*-search diagram of V345 Cas. The dash line indicates the global minimum of $\Sigma W(O-C)^2$ at $T = 7400$ K for the case with a radiative envelope. (b) The *q*-search diagram of V345 Cas. An arrow indicates the global minimum at $q = 0.5$.

Table 3. The photometric solutions of V345 Cas.

Parameter	2007	2008	Weighted Mean
q	0.490(2)	0.498(2)	0.494(2)
$i\,(deg)$	88.55(17)	88.19(17)	88.37(17)
$T_1\,(K)$		7400	
$T_2\,(K)$	4960(9)	4957(7)	4958(8)
Ω_1	3.253(2)	3.247(3)	3.251(2)
$\Omega_2 = \Omega_{in}$	2.860	2.871	2.866
$L_1/(L_1+L_2)_b$	0.9428	0.9430	0.9429
$L_1/(L_1+L_2)_v$	0.9005	0.9008	0.9007
$L_1/(L_1+L_2)_r$	0.8601	0.8605	0.8603
$L_1/(L_1+L_2)_i$	0.8215	0.8219	0.8217
$r_1\,(pole)$	0.3585(4)	0.3598(4)	0.3592(4)
$r_1\,(point)$	0.3979(7)	0.4005(8)	0.3991(7)
$r_1\,(side)$	0.3720(4)	0.3736(5)	0.3727(4)
$r_1\,(back)$	0.3850(6)	0.3870(6)	0.3860(6)
$r_1\,(volume)$	0.3722	0.3739	0.3731
$r_2\,(pole)$	0.2984(3)	0.2994(3)	0.2989(3)
$r_2\,(point)$	0.4275(13)	0.4287(11)	0.4282(12)
$r_2\,(side)$	0.3114(3)	0.3124(3)	0.3119(3)
$r_2\,(back)$	0.3440(3)	0.3449(3)	0.3445(3)
$r_2\,(volume)$	0.3193	0.3202	0.3198
$Colatitude_2$	32.5	48.6	-
$Longitude_2$	3.6	344.3	-
$Radius_2$	23.5	21.3	-
$T_{spot,2}/T_{local,2}$	0.78	0.78	-
$\Sigma W(O-C)^2$	0.00940	0.00696	-

Table 4. Absolute dimensions of V345 Cas.

Parameter	Primary	Secondary
$M/M_\odot$	1.68(6)	0.83(3)
$R/R_\odot$	1.66(2)	1.43(2)
$L/L_\odot$	7.45(61)	1.10(13)

computed at each iteration from the LD tables given by van Hamme (1993). The options of model atmosphere (Kurucz 1993) and synchronous rotation in the WD program were also adopted. The temperature was fixed as $T_1 = 7400K$ and the mass ratio of $q = 0.5$ was used as an initial value. After the photometric solutions of the 2007 and 2008 light curves were separately obtained, a spot model (cool or hot spots on each of two components) was considered to model a small asymmetry appeared in our light curves. Only a cool spot on the secondary star has satisfactory fits to both 2007 and 2008 light curves.

At this moment a third-light was also included in the WD code, but the resultant values for the third-light in the *BVRI* bandpasses were negligibly small within their assigned errors. Our final photometric solutions of V345 Cas for the 2007 and 2008 light curves were listed in the second and third columns of Table 3, respectively, where two solutions are practically consistent each other. The solid lines in Fig. 2 represent the model light and color curves drawn with the solution parameters in Table 3. The weighted mean values of parameters of two solutions were listed in the fourth column of Table 3 and adopted as our final photometric solution of V345 Cas.

Our solution shows that V345 Cas is a typical semi-detached binary system with the cool secondary component filling it's inner Roche lobe, the mass ratio of $q = 0.49$, the inclination of $i = 88.°2$ and the temperature difference of $\Delta T = 2440$ K between two components. The secondary star has a cool spot with a large radius of about 21° ~ 24° near the neck connecting two stars, which makes the light curves slightly asymmetrical and variable near 0.5 phase.

Using the mean solution parameters in Table 3, the Harmanec's (1988) main-sequence relationship between temperature and mass and some well-established relations (Flower 1996, Hilditch 2001, Torres 2010), the absolute dimensions and related radiative parameters of V345 Cas were calculated and listed in Table 4. The luminosities and the bolometric magnitudes were computed by adopting $T_\odot$ =5780 K and $M_{bol\odot} = +4.^m69$ given by Popper (1980). Fig. 4 shows the Roche geometry of V345 Cas where the spectral types of two components are deduced from the table of Cox (2000).
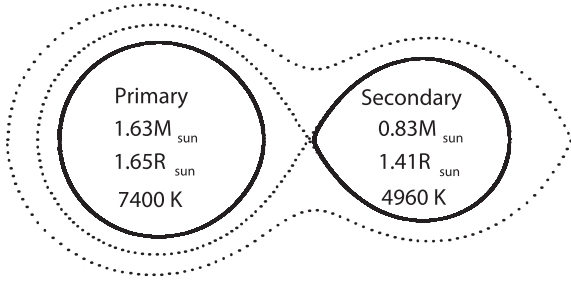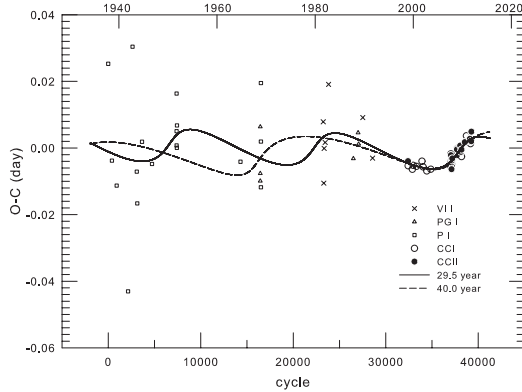
Fig. 4. The Roche geometry of V345 Cas.

Fig. 5. The eclipse timing diagram of V345 Cas. The solid and dashed curves represent the light-time orbits with two possible periods of 29.5 and 40.0 years, respectively.

4. PERIOD STUDY

From our LOAO observations and Super Wide Angle Search for Planets (Butters et al. 2010, Street et al. 2003) measurements, new 14 times of minimum light were determined with the method of Kwee & van Woerden (1956). A total of 69 times of minima, including ours, were collected from the recent database of Kreiner et al. (2001) and from recent literatures. These minima were listed in Table 5 and analyzed to figure out the dynamical behavior of V345 Cas for the first time. An eclipse timing diagram constructed with the Kreiner et al.'s ephemeris was shown in Fig. 5 which contains a timing history of V345 Cas over 66 years. The period change prior to 1990 is not impressive due to large scatter of the residuals of earlier non-CCD minima. However, it is clearly seen that the period, after 1990, is changing in a cyclical pattern, owing to recent high precision CCD minima. Under the assumption that the period change is due to the light-time effect (LITE) by a third-body, all the timings were fitted to an LITE ephemeris as follows:

$$C = T_0 + PE + \tau_3 \qquad (2)$$

Table 5. Observed times of minimum light for V345 Cas.

HJD	Error	Epoch	O-C	Me*	Type	Reference
2,428,835.3360	-	0.0	0.0253	P	I	Götz et al. (1957)
2,429,111.4990	-	401.0	-0.0038	P	I	Götz et al. (1957)
2,429,463.4470	-	912.0	-0.0113	P	I	Götz et al. (1957)
2,430,313.3430	-	2146.0	-0.0431	P	I	Götz et al. (1957)
2,430,645.3980	-	2628.0	0.0304	P	I	Götz et al. (1957)
2,430,957.3680	-	3081.0	-0.0071	P	I	Götz et al. (1957)
2,431,001.4390	-	3145.0	-0.0166	P	I	Götz et al. (1957)
2,431,353.4130	-	3656.0	0.0019	P	I	Götz et al. (1957)
2,432,092.4440	-	4729.0	-0.0048	P	I	Götz et al. (1957)
2,433,922.4960	-	7386.0	0.0163	P	I	Götz et al. (1957)
2,433,924.5510	-	7389.0	0.0051	P	I	Götz et al. (1957)
2,433,926.6130	-	7392.0	0.0008	P	I	Götz et al. (1957)
2,433,947.2750	-	7422.0	0.0000	P	I	Götz et al. (1957)
2,433,949.3480	-	7425.0	0.0068	P	I	Götz et al. (1957)
2,438,680.4180	-	14294.0	-0.0041	P	I	Häussler (1990)
2,440,149.5500	-	16427.0	0.0064	PG	I	Häussler (1990)
2,440,151.6000	-	16430.0	-0.0099	PG	I	Häussler (1990)
2,440,152.2910	-	16431.0	-0.0077	PG	I	Häussler (1990)
2,440,201.2200	--	16502.0	0.0195	P	I	Häussler (1990)
2,440,203.2550	-	16505.0	-0.0118	P	I	Häussler (1990)
2,440,205.3350	-	16508.0	0.0020	P	I	Häussler (1990)
2,444,847.5720	-	23248.0	0.0079	VI	I	Locher (1981a)
2,444,883.3690	-	23300.0	-0.0106	VI	I	Locher (1981b)
2,444,910.2410	-	23339.0	-0.0001	VI	I	Locher (1981b)
2,444,989.4500	-	23454.0	0.0017	VI	I	Locher (1982a)
2,445,241.5530	-	23820.0	0.0191	VI	I	Locher (1982b)
2,447,087.4030	-	26500.0	-0.0032	PG	I	Häussler (1990)
2,447,437.3000	-	27008.0	0.0046	PG	I	Häussler (1990)
2,447,470.3570	-	27056.0	0.0012	PG	I	Häussler (1990)
2,447,788.5713	-	27518.0	0.0092	VI	I	Mikulášek et al. (1992)
2,448,512.4441	-	28569.0	-0.0030	VI	I	Zejda (1995)
2,451,156.2420	0.0020	32407.5	-0.0040	CCD	II	Diethelm (1999)
2,451,166.2276	0.0005	32422.0	-0.0054	CCD	I	Diethelm (1999)
2,451,484.4329	0.0045	32884.0	-0.0064	CCD	I	Šafář & Zejda (2002)
2,451,535.4022	0.0026	32958.0	-0.0052	CCD	I	Šafář & Zejda (2002)
2,451,783.3549	0.0020	33318.0	-0.0055	CCD	I	Brát et al. (2007)
2,452,197.3002	0.0026	33919.0	-0.0040	CCD	I	Brát et al. (2007)
2,452,279.2607	0.0005	34038.0	-0.0057	CCD	I	Diethelm (2002)
2,452,548.5640	0.0003	34429.0	-0.0069	CCD	I	Diethelm (2003)
2,452,856.4395	-	34876.0	-0.0064	CCD	I	Brát et al. (2007)
2,454,316.6084	0.0008	36996.0	-0.0051	CCD	I	This paper (Super WASP)
2,454,344.5060	0.0024	37036.5	-0.0022	CCD	II	This paper (Super WASP)
2,454,345.5370	0.0010	37038.0	-0.0044	CCD	I	This paper (Super WASP)
2,454,347.6059	0.0004	37041.0	-0.0018	CCD	I	This paper (Super WASP)
2,454,349.6684	0.0006	37044.0	-0.0055	CCD	I	This paper (Super WASP)
2,454,382.3855	0.0007	37091.5	-0.0044	CCD	II	Hübscher et al. (2008)
2,454,394.4384	0.0010	37109.0	-0.0048	CCD	I	This paper (Super WASP)
2,454,396.5059	0.0028	37112.0	-0.0036	CCD	I	This paper (Super WASP)
2,454,396.8475	0.0010	37112.5	-0.0064	CCD	II	This paper (LOAO)
2,454,404.7716	0.0000	37124.0	-0.0029	CCD	I	This paper (LOAO)
2,454,440.2419	0.0011	37175.5	-0.0037	CCD	II	Hübscher et al. (2009a)
2,454,453.6736	0.0002	37195.0	-0.0028	CCD	I	This paper (LOAO)
2,454,454.7064	0.0005	37196.5	-0.0031	CCD	II	This paper (LOAO)
2,454,758.7943	0.0001	37638.0	-0.0020	CCD	I	This paper (LOAO)
2,454,778.7686	0.0001	37667.0	-0.0017	CCD	I	This paper (LOAO)
2,454,779.8033	0.0003	37668.5	-0.0001	CCD	II	This paper (LOAO)
2,454,798.3995	0.0015	37695.5	-0.0005	CCD	II	Hübscher et al. (2009b)
2,455,039.4661	0.0005	38045.5	0.0007	CCD	II	Hübscher et al. (2010)
2,455,097.3199	0.0011	38129.5	-0.0012	CCD	II	Hübscher et al. (2010)
2,455,139.6771	0.0003	38191.0	-0.0026	CCD	I	Diethelm (2010)
2,455,141.4011	0.0021	38193.5	-0.0005	CCD	II	Hübscher et al. (2010)
2,455,380.4025	0.0003	38540.5	0.0018	CCD	II	Hübscher et al. (2011)
2,455,502.6590	0.0006	38718.0	0.0037	CCD	I	Diethelm (2011)
2,455,758.5318	0.0025	39089.5	0.0028	CCD	II	Hübscher et al. (2012)
2,455,808.4653	0.0008	39162.0	0.0013	CCD	I	Hübscher & Lehmann (2012)
2,455,815.3537	0.0010	39172.0	0.0021	CCD	I	Hübscher & Lehmann (2012)
2,455,839.4607	0.0003	39207.0	0.0025	CCD	I	Hübscher & Lehmann (2012)
2,455,868.7324	0.0004	39249.5	0.0020	CCD	II	Diethelm (2012)
2,455,873.5566	0.0064	39256.5	0.0049	CCD	II	Hübscher & Lehmann (2012)

*P: plate, PG: photographic, VI: visual : CCD: charge-coupled device

where τ_3 is the LITE term of which the details were given by Irwin (1952). The seven unknown parameters in Eq. (3)

Table 6. The solution of Eq. (2) for V345 Cas.

Parameter	Short period	Long period	Unit
T_0	2451166.2319 (11)	2451166.2318 (12)	HJD
P	0.68875825 (12)	0.68875840 (12)	day
$a_{12} \sin i_3$	0.993 (91)	1.16 (17)	AU
K	0.0050	0.0055	day
ω_3	9.57 (38)	338 (22)	deg
e_3	0.51 (17)	0.61 (12)	
P_3	29.5 (1.3)	40.0 (1.4)	Year
T_3	2455011 (298)	2454495 (307)	HJD
σ	0.003564	0.003627	day

(Irwin 1959) were determined with a Levenberg-Marquardt method (Press et al. 1992) which was frequently used by the authors (e.g., Kim et al. 2010, Jeong & Kim 2011, Kim & Jeong 2012). The result shows that two solutions rather than an unique solution are possible in parallel mainly because the time-span of the CCD timing data with high precision is short while non-CCD minima with longer time-span have large scatters. As listed in Table 6, the one LITE solution has P_3 = 29.5 yr, e = 0.61, and K = 0.0055 d and the other P_3 = 40.0 yr, e = 0.51, and K = 0.0050 d. The 1-σ value of the solution for the shorter period is slightly smaller than that for the longer one, however, the difference is so small that we can not decern, at the moment, which one between two solutions is more realistic. More timings would be needed to resolve the ambiguity in the secondary periods for the cyclical period change. Solid and dashed curves in Fig. 5 denote the shorter and longer LITE solutions, respectively. When two cyclical period changes suggested here are assumed to be caused by the Applegate (1992) mechanism in the convective region of the late-type secondary star, the resultant Applegate parameters are quite small (e.g., $2 \times 10^{-2} < \Delta L_s / L_s < 4 \times 10^{-2}$), indicating that the Applegate model could not work well.

5. DISCUSSION AND CONCLUSION

In order to investigate the evolutionary status of each of components of V345 Cas, mass-radius and mass-luminosity diagrams for the components of V345 Cas together with six other short-period Algol binaries were
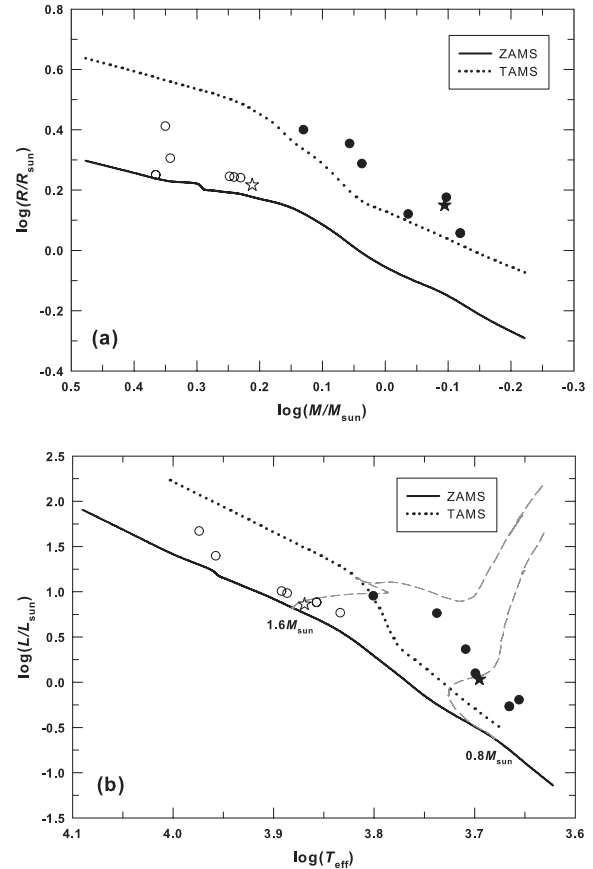

Fig. 6. The HR diagrams of some short-period Algol binary stars. (a) The mass-radius diagram. (b) The temperature-luminosity diagram. The open and filled symbols represent the primary and secondary components. Two components of V345 Cas were designated as star symbols. The thick solid and dotted lines represent the beginning (ZAMS) and ending (TAMS) phases of core hydrogen burning, respectively, which were calculated with the Giradi et al.'s (2000) evolutionary stellar models for Population I stars (X = 0.708, Y = 0.273, Z = 0.019). Two evolutionary tracks corresponding to 1.6 and 0.8 $M_\odot$ were also drawn as short-dashed lines in the temperature-luminosity diagram.

drawn in the upper and lower parts of Fig. 6, respectively. The information on stellar parameters of other binaries was listed in Table 7. In the figure, open and filled star symbols represent the primary and secondary components of V345 Cas, respectively, while the primary and secondary components of other binary stars are designated as open and filled circles, respectively. The thick solid and dotted

Table 7. Absolute dimensions of some short-period Algol binary stars.

Star	Period (day)	$M_1/M_\odot$	$M_2/M_\odot$	$R_1/R_\odot$	$R_2/R_\odot$	$T_1 (K)$	$T_2 (K)$	$L_1/L_\odot$	$L_2/L_\odot$	Ref.*
CL Aur	1.2444	2.24	1.35	2.58	2.51	9420	6323	46.96	9.02	1
GW Gem	0.6594	1.74	0.80	1.75	1.50	7700	5004	9.65	1.26	2
SW Lyn	0.6441	1.77	0.92	1.76	1.32	7800	4528	10.15	0.64	3
KZ Pav	0.9499	1.70	1.09	1.74	1.94	6820	5116	5.86	2.32	4
V505 Sgr	1.1829	2.20	1.14	2.02	2.26	9070	5466	25.00	5.80	5
RU UMi	0.5249	2.32	0.76	1.78	1.14	7200	4630	7.63	0.54	6

*1: Lee et al. (2010), 2: Lee et al. (2009), 3: Kim et al. (2010), 4: Sürgit et al. (2010), 5: İbanoğlu et al. (2000), 6: Lee et al. (2008)

lines represent the beginning (ZAMS) and ending (TAMS) phases of core hydrogen burning, respectively, which were calculated with the Girardi et al.'s (2000) evolutionary stellar models for Population I stars ($X = 0.708$, $Y = 0.273$, $Z = 0.019$). Two evolutionary tracks corresponding to 1.6 and 0.8 $M_\odot$ were also drawn in the mass-luminosity diagram. As shown in the figures, the components of V345 Cas are located on the positions that the primary is in slightly upper region from the ZAMS while the secondary is located in the sub-giant domain, which is similar to other short-period Algols, indicating that the primary star is a A7 main-sequence star but the secondary is an evolved K3 sub-giant star. The ratio of the primary star's radius to it's Roche volume radius is about 0.85. Therefore, V345 Cas is not a near-contact binary and would be expected to evolve into the near-contact stage.

Although the photometric properties of V345 Cas were comprehensively understood by our study, however the details are far from the reality. The lack of the present timing data can not constrain any secular period change which would be expected from the semi-detached configuration of the system and resulted in two possible secondary periods for a cyclical period change. More photometric and spectroscopic observations are needed to resolve what we have suggested as some problems and further to improve the understanding of the system.

ACKNOWLEDGMENTS

REFERENCES

Applegate JH, A mechanism for orbital period modulation in close binaries, ApJ, 385, 621-629 (1992). http://dx.doi.org/10.1086/170967

Brát L, Zejda M, Svoboda P, B.R.N.O. Contributions 34, OEJV, 74, 1-75 (2007).

Butters OW, West RG, Anderson DR, Collier Cameron A, Clarkson WI, et al., The first WASP public data release, A&A, 520, L10, 1-4 (2010). http://dx.doi.org/10.1051/0004-6361/201015655

Cox AN, Allen's Astrophysical Quantities, fourth edition, ed., A. N. Cox (Springer, New York, 2000), 151, 388.

Diethelm R, 152. List of Minima of Eclipsing Binaries, BBSAG Bull., 119, 1-10 (1999).

Diethelm R, 160. List of Minima of Eclipsing Binaries, BBSAG Bull., 127, 1-11 (2002).

Diethelm R, 162-nd list of minima timings of eclipsing binaries by BBSAG observers, IBVS, No. 5438, 1-11 (2003).

Diethelm R, Timings of Minima of Eclipsing Binaries, IBVS, No. 5920, 1-7 (2010).

Diethelm R, Timings of Minima of Eclipsing Binaries, IBVS, No. 5960, 1-11 (2011).

Diethelm R, Timings of Minima of Eclipsing Binaries, IBVS, No. 6011, 1-13 (2012).

Flower PJ, Transformations from Theoretical Hertzsprung-Russell Diagrams to Color-Magnitude Diagrams: Effective Temperatures, B-V Colors, and Bolometric Corrections, ApJ, 469, 355-365 (1996).

Götz W, Huth H, Hoffmeister C, Die Veraenderlichen Sterne der nordlichen Milchstrasse Teil IX, VeSon, 4, 123-238 (1957).

Girardi L, Bressan A, Bertelli G, Chiosi C, Evolutionary tracks and isochrones for low- and intermediate-mass stars: From 0.15 to 7 $M_\odot$, and from Z = 0.0004 to 0.03, A&AS, 141, 371-383 (2000). http://dx.doi.org/10.1051/aas:2000126

Harmanec P, Stellar masses and radii based on modern binary data, Bull. Astron. Inst. Czech., 39, 329-345 (1988).

Häussler K, Veranderliche im Feld 23^h 09^m $+52°5$ (supplement), VeSon, 10, 374-388 (1990).

Hilditch RW, An Introduction to Close Binary Stars (Cambridge University Press, Cambridge, 2001), Chap. 6.

Hoffmeister C, 213 neue Veranderliche, AN, 274, 36-40 (1943).

Huth H, Herausgegeben von der sternwarte Sonneberg der Deutschen Akademie der Wissenschaften, MVS, 229 (1956).

Hübscher J, BAV-results of observations-photoelectric minima of selected eclipsing binaries and maxima of pulsating stars, IBVS, 5984, 1-16 (2011).

Hübscher J, Lehmann PB, BAV-Results of Observations-Photoelectric Minima of Selected Eclipsing Binaries and Maxima of Pulsationg Stars, IBVS, No. 6026, 1-23 (2012).

Hübscher J, Lehmann PB, Monninger, G, Steinbach H-M, Walter F, BAV-results of observations-photoelectric minima of selected eclipsing binaries and maxima of pulsating stars, IBVS, No. 5941, 1-16 (2010).

Hübscher J, Lehmann PB, Walter F, BAV-Results of Observations-Photoelectric Minima of Selected Eclipsing Binaries and Maxima of Pulsationg Stars, IBVS, No. 6010, 1-22 (2012).

Hübscher J, Steinbach H-M, Walter F, BAV-Results of Observations-Photoelectric Minima of Selected Eclipsing Binaries and Maxima of Pulsationg Stars, IBVS, No. 5830, 1-8 (2008).

Hübscher J, Steinbach H-M, Walter F, BAV-Results of Observations-Photoelectric Minima of Selected Eclipsing Binaries and Maxima of Pulsationg Stars, IBVS, No. 5874, 1-13 (2009a).

Hübscher J, Steinbach H-M, Walter F, BAV-results of observations-photoelectric minima of selected eclipsing binaries and maxima of pulsating stars, IBVS, No. 5889, 1-13 (2009b).

Irwin JB, The determination of a light-time orbit, ApJ, 116, 211-217 (1952). http://dx.doi.org/10.1086/145604

Irwin JB, Standard light-time curves, AJ, 64, 149-155 (1959). http://dx.doi.org/10.1086/107913

İbanoğlu C, Çakirli Ö, Değirmenci Ö, Saygan S, Ulaş B, et al., The BV light and it O-C curves analyses of the triple system V505 Sagittarii, A&A, 354, 188-192 (2000).

Jeong JH, Kim C-H, WZ Cephei: a dynamically active W UMa-type binary star, JASS, 28, 163-172 (2011). http://dx.doi.org/10.5140/JASS.2011.28.3.163

Kim C-H, Jeong JH, V700 Cygni: A Dynamically Active W UMa-type Binary Star II, JASS, 29, 151-161 (2012).

Kim C-H, Kim H-I, Yoon TS, Han W, Lee JW, et al., SW Lyncis-advances and questions, JASS, 27, 263-278 (2010). http://dx.doi.org/10.5140/JASS.2010.27.4.263.

Kreiner JM, Kim C-H, Nha IS, An atlas of O-C diagrams of eclipsing binary stars (Wydawnictwo Naukowe Akademii Pedagogicznej, Krakow, 2001).

Kurucz RL, in Light Curve Modeling of Eclipsing Binary Stars, ed., E. F. Milone (Springer-Verlag, New York, 1993), 93.

Kwee KK, van Woerden H, A method for computing accurately the epoch of minimum of an eclipsing variable, BAN, 12, 327-330 (1956).

Lee JW, Kim C-H, Kim DH, Kim S-L, Lee CU, et al., The First Comprehensive Photometric Study of the Algol-type System CL Aurigae, AJ, 139, 2669-2678 (2010). http://dx.doi.org/10.1088/0004-6256/139/6/2669

Lee JW, Kim C-H, Kim S-L, Lee C-U, Han W, et al., A Long-term Photometric Study of the Near-contact Binary RU Ursae Minoris, PASP, 120, 720-729 (2008).

Lee JW, Kim SL, Lee CU, Kim HI, Park JH, et al., Photometric Properties of the Near-Contact Binary GW Geminorum, PASP, 121, 114-110 (2009).

Locher K, 89th List of Minima of Eclipsing Binaries, BBSAG Bull., 56, 1-7 (1981a).

Locher K, 90th List of Minima of Eclipsing Binaries, BBSAG Bull., 57, 1-7 (1981b).

Locher K, 91th List of Minima of Eclipsing Binaries, BBSAG Bull., 58, 1-7 (1982a).

Locher K, 95th List of Minima of Eclipsing Binaries, BBSAG Bull., 62, 1-7 (1982b).

Lucy LB, Gravity-Darkening for Stars with Convective Envelopes, ZA, 65, 89-92 (1967).

Mikulášek Z, Šilhán J, Zejda M, Contributions Nicholas Copernicus Observatory, Brno, 30, 4 (1992).

Monet DG, Levine SE, Canzian B, Ables HD, Bird AR, et al., The USNO-B catalog, AJ, 125, 984-993 (2003).

Popper DM, Stellar masses, ARA&A, 18, 115-164 (1980).

Press WH, Teukolsky SA, Vetterling WT, Flannery BP, Numerical recipes in C, 2nd ed. (Cambridge University Press, Cambridge, 1992), Chap. 15.

Rucinski SM, The Proximity Effects in Close Binary Systems. II. The Bolometric Reflection Effect for Stars with Deep Convective Envelopes, AcA, 19, 245-255 (1969).

Šafář J, Zejda M, CCD times of minima of faint eclipsing binaries III, IBVS, No. 5263, 1-9 (2002).

Sipahi E, 2004 UBVR Photometry of the Eclipsing Binary KR Cyg, IBVS, No. 5635, 1-4 (2005).

Street RA, Pollaco DL, Fitzsimmons A, Keenan FP, Horne K, et al, SuperWASP: Wide Angle Search for Planets, ASPC, 294, 405-408 (2003).

Sürgit D, Erdem A, Budding E, The Algol binary system KZ Pavonis revisited, MNRAS, 407, 497-506 (2010).

Torres G, On the Use of Empirical Bolometric Corrections for Stars, AJ, 140, 1158-1162 (2010).

van Hamme W, New limb-darkening coefficients for modeling binary star light curves, AJ, 106, 2096-2117 (1993).

van Hamme W, Wilson RE, Stellar atmospheres in eclipsing binary models, ASPC, 298, 323-328 (2003).

Wilson RE, Biermann P, TX CANCRI - Which component is hotter, A&A, 48, 349-357 (1976).

Wilson RE, Devinney EJ, Realization of accurate close-binary light curves: application to MR Cygni, ApJ, 166, 605-619 (1971). http://dx.doi.org/10.1086/150986

Zejda M, Contributions Nicholas Copernicus Observatory, Brno, 31, 4 (1995).